

The Spectral Energy Distribution Camera for the LMT

G.W. Wilson^a, T.C. Chen^b, E.S. Cheng^c, D.A. Cottingham^b, T. Crawford^d,
D.J. Fixsen^e, F.M. Finkbeiner^e, D.W. Logan^a, S. Meyer^d,
R.F. Silverberg^c, and P.T. Timbie^f

^aUniversity of Massachusetts, Dept. of Astronomy, Amherst, MA, 01003, U.S.A.

^bGlobal Science and Technology, NASA GSFC LASP, Greenbelt, MD, U.S.A.

^cNASA GSFC Laboratory for Astronomy and Solar Physics, Greenbelt, MD, U.S.A.

^dEnrico Fermi Institute, University of Chicago, Chicago, IL, U.S.A.

^eSSAI, NASA GSFC LASP, Greenbelt, MD, U.S.A.

^fUniv. of Wisconsin, Department of Physics, Madison, WI, U.S.A.

ABSTRACT

Advances in bolometer device and readout technologies make it possible to build photon-noise limited bolometric cameras for ground-based observations at mm-wave frequencies. However, today's bolometer cameras are limited not by photon-noise of the telescope and atmosphere but by fluctuations in the atmosphere signal. To realize the full potential of bolometer cameras on large aperture ground-based telescopes, one must find a way to defeat this foreground.

The SPECTral Energy Distribution Camera - or SPEED - is a four pixel, four frequency camera planned for eventual use on the Large Millimeter Telescope (LMT). A prototype version of this camera is currently being built for initial operation on the Heinrich Hertz Telescope (HHT). SPEED incorporates Frequency Selective Bolometers to sample the sky with a frequency-independent beam simultaneously at four frequencies (from 150 to 375 GHz) in each pixel. SPEED's ability to separate the temporally varying atmospheric signal from the true sky signal will potentially result in a per-detector sensitivity between 2 and 5 times greater than that achieved with contemporary bolometer cameras. We describe the basic design and motivation for SPEED, the expected sensitivity of the camera on the LMT, and give examples of some of the science programs we will undertake.

Keywords: Bolometer Camera, FIR Detectors, Cosmology, HHT, LMT

1. INTRODUCTION

The detection of high redshift galaxies by the SCUBA team¹ and the mapping of the Sunyaev Zel'dovich effect (SZE) in a number of clusters by the BIMA and OVRO arrays² have sparked an interest in multi-pixel bolometric cameras in the radio-astronomy community. In fact, several ground-based telescopes have commissioned or are planning to build bolometric focal plane arrays for making continuum observations. These include the SCUBA and SCUBA2 arrays on the JCMT, the BOLOCAM array on the CSO, the MAMBO array on the IRAM 30 meter telescope, and the BOLOCAM II array for the Large Millimeter Telescope (LMT). The combination of these sensitive bolometric arrays with the high resolution and large field of view of these telescopes has enormous promise. BOLOCAM II on the LMT, for example, will map tens of square degrees at its confusion limit at 1mm wavelength - revealing hundreds to thousands of previously undetected protogalaxies with each hour of observation.

Bolometer arrays promise large improvements in sensitivity over single pixel bolometer systems for two reasons: 1) the total raw system sensitivity scales as $\sqrt{N_{\text{pix}}}$ and 2) for ground-based observations limited primarily by noise from the fluctuating atmosphere, a closely spaced array provides the ability to remove some

Direct correspondence to G.W.W.

E-mail: wilson@astro.umass.edu

Telephone: 1 413 545 0460

of the coherent sky noise due to variation in the sky emission as the water vapor column density varies. Large bolometer arrays, on the other hand, are usually limited to operation at a single wavelength. While, in general, this is not a disadvantage for the detection of objects, multi-spectral interrogation must be accomplished with subsequent observations with other instruments or instrument configurations.

The SPECTral Energy Distribution (SPEED) Camera is a small format bolometer camera designed to complement existing and planned wide format bolometer arrays by providing a means to quickly and efficiently study previously identified sources. Using the new technology of frequency selective bolometers, SPEED simultaneously samples the mm-wave spectral energy distribution (SED) in four frequency bands in each of four pixels. A prototype version of the SPEED camera is currently being built for initial use on the Heinrich Hertz Telescope (HHT). A copy of this instrument will be built for use on the 50m diameter Large Millimeter Telescope. In conjunction with BOLOCAM II on the LMT, SPEED will be used to measure the mm-wave SED of a variety of previously unknown sources including protogalaxies, clusters exhibiting the Sunyaev-Zel'dovich effect, and various galactic sources.

2. INSTRUMENT DESIGN

SPEED is a four pixel multi-frequency camera for use on millimeter telescopes. The camera is designed to observe the sky simultaneously at 2, 1.3, 1.1, and 0.85 mm via frequency selective bolometers (FSBs). SPEED's photometer will operate at 270mK (cooled by a ^3He refrigerator) and will require several filters to suppress out of band radiation. Voltage-biased transition edge superconducting (TES) thermistors provide stability and sensitivity for detecting cosmic signal. The sixteen detectors are then read through a SQUID multiplexing circuit. By combining four FSBs in series and multiplexing the output, SPEED offers a compact, reliable instrument for mm astronomy.

2.1. Detector Passbands

While ground-based telescopes enjoy a relatively low-cost and large degree of convenience over sub-orbital and orbital payloads, a large price is paid at mm wavelengths in instrument sensitivity and available observing time due to emission and absorption by the Earth's atmosphere. Placing instruments at high altitudes above most of the atmosphere lessens the impact from the sky but millimeter observing is still reduced to a few semi-transparent windows.

Figure 1 shows a model³ of the effective temperature of the atmosphere between 100 and 500 GHz at the LMT site. The saturated lines in this waveband arise from oxygen and water vapor in the atmosphere. The complexity of the atmosphere imposes constraints upon the bandpass of any millimeter instrument. SPEED aims at detecting the maximum possible signal within the windows of transmission while simultaneously rejecting the large emission due to the saturated atmospheric lines. This is accomplished by incorporating Frequency Selective Bolometers, notch filters, and by carefully controlling stray light in the optical system. The result of this combination is a highly-sensitive multi-spectral band photometer with a higher per-detector sensitivity than any existing ground-based bolometer camera.

2.1.1. Frequency Selective Bolometers

An FSB is a bolometer incorporated into a quasi-optical interference filter. The chief advantage of using an FSB is that different frequency FSBs can be cascaded together in a common light pipe to produce a multifrequency photometer in a compact configuration.⁴ Each FSB is formed from two similar elements, a bolometer and a backshort, that behave as a resonant structure designed to be maximally absorptive over a narrow bandwidth and maximally transmissive at all other frequencies. Figure 2 shows an exploded view of a potential geometry of the SPEED photometer made up of FSBs mounted in 10mm diameter lightpipe. Details on the design and fabrication techniques used to create FSB detectors can be found in Cottingham *et al.*⁵ in these proceedings.

The SPEED FSB optical design is optimized by modeling the FSB response with Agilent HFSS. A discussion of the FSB model and its comparison with measurements can be found in Cottingham *et al.*⁵ in these proceedings. The HFSS model has been tested with a number of prototype optical designs and has been shown to accurately

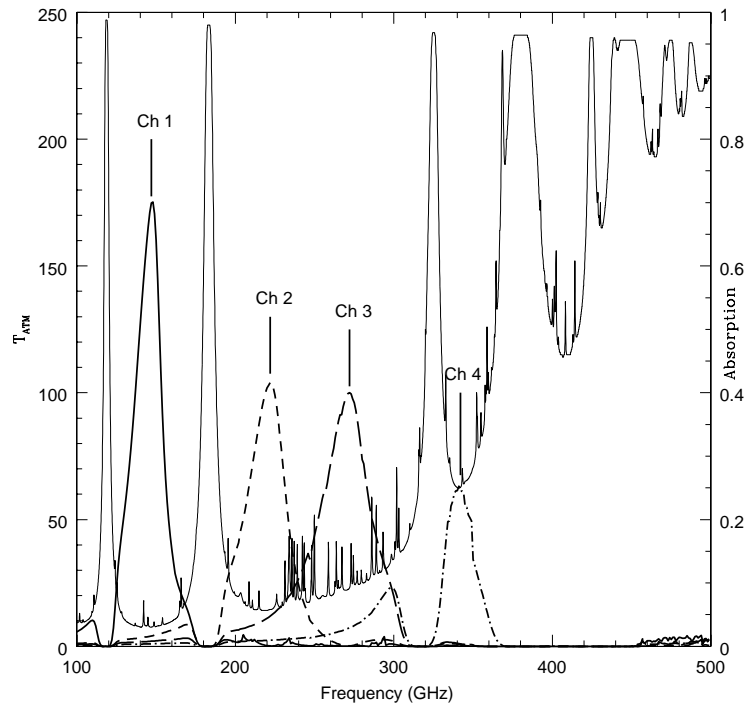


Figure 1. Model of the effective atmospheric temperature with 2 mm of precipital water vapor at the LMT site. Overlaid on the model are the predicted SPEED passbands.

reproduce their transmission spectra when measured with a Fourier Transform Spectrometer at the University of Chicago. We are currently awaiting the results of the first round of testing of SPEED devices.

Figure 3 displays the model 2 mm channel from SPEED overlaid with two notch filters (see Sect. 2.1.2) and the effective atmospheric temperature. Despite its location behind two other filters, the bolometer absorbs nearly 80% of the resonant radiation at 145 GHz. The advantage of FSBs is apparent when all four bolometers, four notch filters, and two lowpass filters are cascaded together; the 145 GHz channel still absorbs over 70% of the incident radiation. The three sharp troughs at 165, 185, and 205 GHz are artifacts of the HFSS modeling software. Actual devices measured up to 1 THz do not show these sharp features.

2.1.2. Notch Filters

A challenge with ground-based instrument development in the millimeter waveband is the restriction of observing through windows of transmission. One solution to the problem of atmospheric lines is to include optical elements that operate as notch filters. These filters are designed to remove signal in narrow bands that contain the saturated line and reduce the background loading on the bolometer elements. SPEED's optics contain four such notch filters. Centered at 120, 185, 325 and 380 GHz, the notch filters are designed much like a pair of FSB backshorts. Each notch filter acts as a resonant structure to destructively interfere the signal from the oxygen and water lines. The notch filters are placed in the same light pipe directly in front of the FSBs at 270mK. Like the ordering of the FSBs, the notch filters are cascaded from highest resonant frequency to lowest.

We have extensively modeled the spectral behavior of a range of notch filters. The quality of each notch filter can be evaluated quantitatively by determining the atmospheric power absorbed by each bolometer. The incident power from the atmosphere is given by:

$$\mathbf{P}_{sky} = \varepsilon_{sky} \varepsilon \mathbf{A} \Omega \int_0^{\infty} \mathbf{B}_{\nu}(\mathbf{T}) f(\nu) d\nu \quad (1)$$

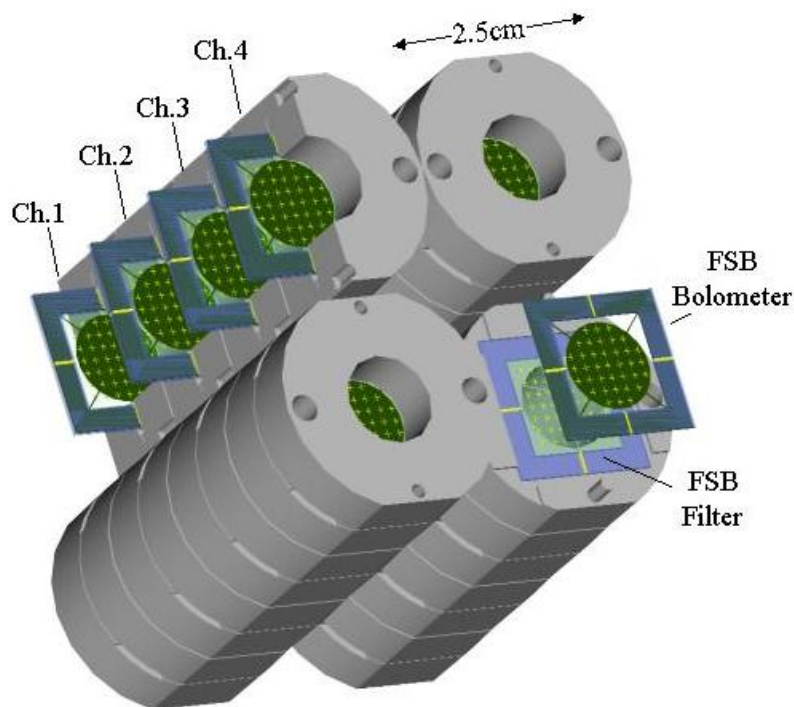


Figure 2. An exploded cartoon view of a possible four pixel photometer configuration for SPEED. The final photometer configuration will depend on some parameters of device processing which are being explored at the time of this writing. Notch filters and low-pass filters are not shown. Four FSB channels absorb in atmospheric windows at 2mm, 1.5mm (two channels), and 0.85mm.

where the emissivity of the atmosphere is ϵ_{sky} , the optical efficiency, ϵ , is set to unity, the étendue, $\mathbf{A}\Omega$, equals $4.5 \text{ mm}^2 \text{ sr}$, and $\mathbf{f}(\nu)$ is the modeled bolometer's effective bandpass including the upstream detectors and notch filters.

To illustrate the importance of including notch filters into SPEED's optics, Table 1 shows the power absorbed by a modeled SPEED channel centered in the 2 mm window both with and without suppressing notch filters. Although the total power absorbed from the atmosphere in band (135-170 GHz) does not significantly change with inclusion of two notch filters, the total power absorbed from the saturated water lines drops by 60%.

Table 1. Power absorbed by a SPEED bolometer located at 145 GHz with ϵ_{sky} and ϵ set to unity.

Channel	Total Power	110-125 (GHz)	125-175 (GHz)	175-200 (GHz)
Without Notch Filters	9.66 pW	2.01 pW (21%)	3.58 pW (37%)	4.06 pW (42%)
With Two Notch Filters	3.73 pW	0.14 pW (4%)	3.21 pW (86%)	0.37 pW (10%)

2.1.3. Out of Band Suppression

As a result of early testing and extensive modeling, additional means of high frequency suppression must be included in the optical stream. Although the out of band bolometer response is near zero at frequencies beyond 400 GHz, the combination of low-level out of band leakage of the FSB and high effective atmospheric

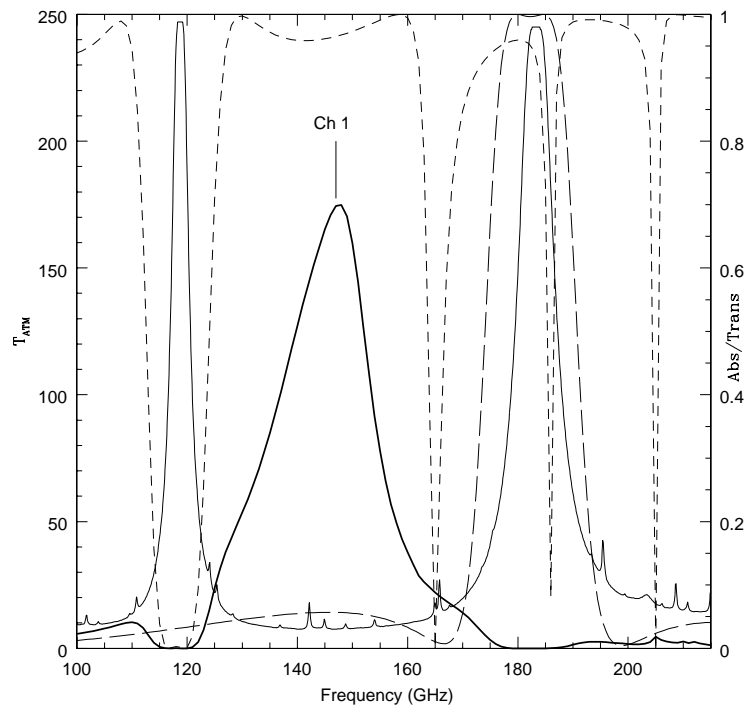


Figure 3. SPEED channel overlaid with a model of the atmosphere with 2 mm of precipitable water vapor. The transmission response of the two adjacent notch filters is shown with dashed lines. The sharp dips in transmission of the notch filters is an artifact of the HFSS model.

temperature requires further suppression of the optical input at high frequencies. Radiation in the infrared spectrum is handled through a series of IR blocking materials such as zotefoam and fluorogold. Frequencies closer to the instrument passband require a sharper filter to reduce the power loading on the bolometers. SPEED's design includes two single pole lowpass filters to reduce the optical loading on the bolometers above 400 GHz.

2.1.4. Cumulative Passbands

The predicted absorption spectrum of each of SPEED's four bands is shown in Figure 1 along with the predicted atmospheric spectrum at the LMT site. Several features of the spectra are noteworthy. First, the existence of the notch filters is evident in the lack of absorption at frequencies where there are saturated water or oxygen lines. As mentioned above, these notch filters are essential in limiting the photon noise and atmosphere fluctuation noise on the detectors.

Second, the channel 4 detector straddles a strong water line (which has been notched out upstream of the FSB) and has significant response inside of the 1.3mm atmospheric window. Because the SPEED FSBs use a single pole filter to generate the bandpass, we found it impossible to center the channel inside of the $0.85\mu\text{m}$ window without suffering significant leakage at higher frequencies. Rather than building a noisy channel, we have chosen to heavily notch the 312GHz water line and live with some extra correlation between channels 3 and 4.

Finally, the reduction in peak optical efficiency with frequency is primarily a result of the two lowpass filters used to reduce the high frequency out of band response. Channel 1's high peak optical efficiency is a testament to the high out of band transmission of the higher frequency channels.

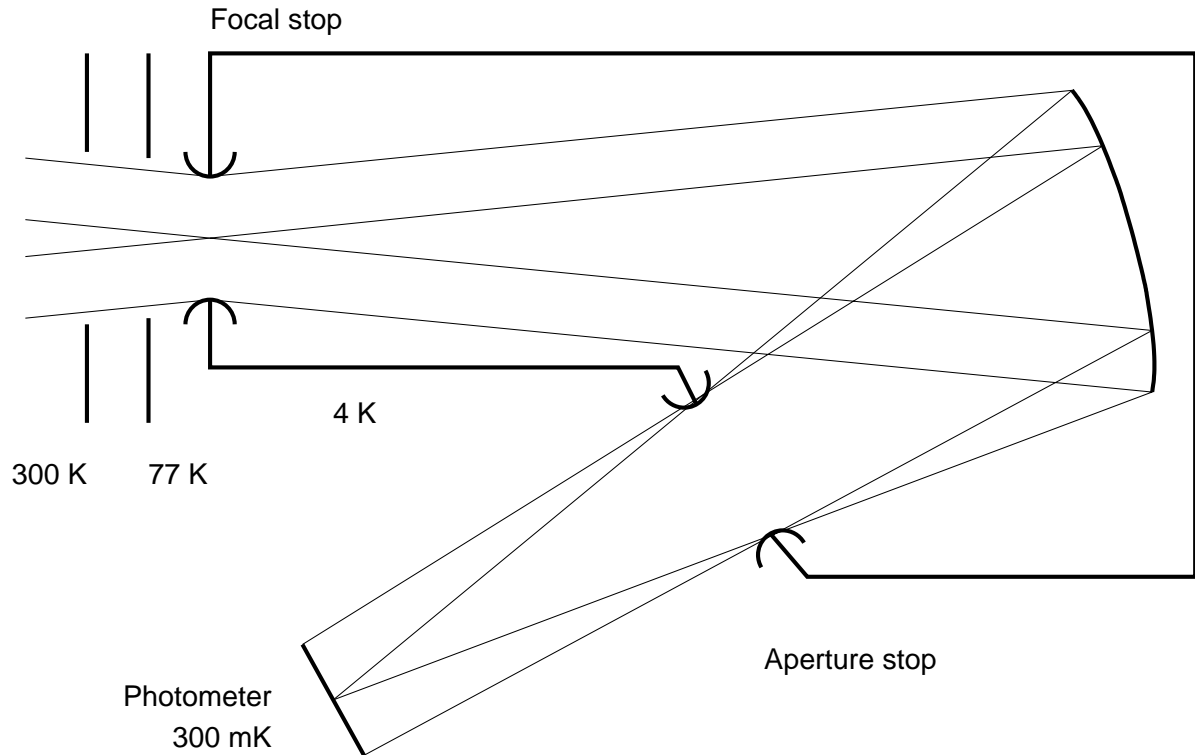


Figure 4. A conceptual view of the optical layout of the SPEED radiometer.

2.2. Telescope Coupling Optics

A conceptual view of the optical layout of SPEED appears in Figure 4. One optic external to the dewar adapts the dewar feed to the feed of the telescope; this optic will be different for HHT and LMT. There is a focal plane where the beam penetrates the 4 K shield of the dewar, and a focal stop is placed here. Optics inside the dewar reimaging this plane onto the detector array (for simplicity, the figure shows just one reimaging optic). Another cold stop, also at 4 K, is placed at an image of the aperture plane. Finally, truncated Winston cones (at 270mK) adapt the ends of the FSB light pipes, which cannot be packed closely enough to fill the focal plane, to a filled focal plane at higher $f/\#$.

The system of reimaging optics and cold stops serves both optical and thermal purposes. Thermally, it prevents any radiation from outside the $A\Omega$ that the instrument observes from reaching the cold stage of the dewar, thus minimizing the radiative load on the refrigerator. Optically, it controls stray light due to diffraction at the edges of the optics in such a way as to minimize primary mirror spillover.

2.3. Thermistor Choice

A transition edge superconducting (TES) detector can be biased at its critical temperature to become an extremely sensitive thermistor. The strengths of using TES devices are the high linearity ($\approx 1\%$)⁶ of the response and the reproducibility of transition temperatures in fabrication.

Each of SPEED's bolometer elements will have two TES devices attached around the periphery of the 1.12 cm suspended SiN membrane. The TES devices are made from bi-layers of molybdenum and gold. Achieving a $T_c \approx 405$ mK is accomplished through varying the thickness of the bi-layers. Each SPEED TES will be 120 nm thick with equal 60 nm thick layers of molybdenum and gold. The two TES devices per bolometer will be wired in series with niobium layered leads ($T_c \approx 9.1K$) approximately 100 nm thick by 5 μm wide.

2.4. Electronics

The TES sensors for the 16 separate detectors will be read out with SQUID multiplexers, following the time-based multiplexing scheme developed at the National Institute of Standards and Technology.^{6,7} We have obtained SQUID multiplexers from Erich Grossman at NIST which will be incorporated into the instrument. While multiplexing is not required to read out 16 detectors, we consider SPEED to be an important stepping stone in learning about future bolometer readout technologies.

3. ATMOSPHERE FLUCTUATION SUBTRACTION

To date, ground-based bolometer cameras have been heavily noise-limited by variation in the sky emission as the water vapor column density varies over the telescope.⁸ As mentioned in Section 1, by using an array, this common-mode contribution to the noise can be subtracted by differencing each pixel with the array average for each integration. For the BOLOCAM instrument on the CSO, for example, this technique reduces the total noise to within a factor of a few of the expected photon noise.⁹

SPEED will take the array advantage one step further. Since the four bands in a given FSB stack all share the same column of atmosphere between the telescope and the sky, any atmospheric fluctuation signal will be common between the channels. Thus, by modulating the sky signal (by chopping or scanning the telescope) in a manner that cleanly separates the fixed sky from the changing atmosphere, a principal component analysis can be made to identify and remove the variable atmosphere signal from the true sky signal. This technique can be thought of as a temporal removal of the atmosphere. Once the temporal removal is done, a spatial removal will be made using the same techniques as a conventional bolometer array.

Note that the temporal removal technique does not require any a priori knowledge of the power spectrum of the fluctuations in the atmosphere. What is required, however, is that the detector passbands not be sensitive to saturated line emission from the atmosphere which will not change in a smooth manner with time. Removing the detector sensitivity to this saturated line emission is the primary motivation behind the notch filters described in Section 2.1.2.

The temporal removal technique reduced the atmospheric fluctuation noise in observations at Mauna Kea in Meyer *et al.*¹⁰ by a factor of 5 and was limited by detector sensitivity. For those observations, a linearized model of water vapor column density fluctuations predicted a reduction of the effects of water vapor column density fluctuations on the measurement of SZ effect of more than a factor 30. For a photon noise limited bolometer system, the sensitivity gain would lie between 5 and 30 due to the non-linearity in the atmospheric emission fluctuations. Ultimately, with the advent of large format multi-pixel, multi-frequency arrays, the analysis will make use of the temporal, spatial and spectral correlation present in the atmospheric noise. These future bolometer arrays will be photon noise limited at reasonably good ground-based sites in spite of atmosphere emission fluctuations – SPEED will serve as an important test bed in this enormous step forward in sensitivity.

4. SENSITIVITY CALCULATIONS

A sensitivity is calculated for each detector in each FSB chain following the bolometer noise nonequilibrium theory by Mather^{11,12} as well as the TES analog by Lee *et al.*¹³ Each detector's noise budget is composed of a combination of thermal noise (resulting from the bolometer's weak thermal link to the bath), Johnson noise (from the thermistor), and photon noise (due to the random fluctuations in the number of photons absorbed per unit time). Of the three, the thermal and Johnson noise contributions are the most accurately calculated and are intrinsic to the detector design. Unfortunately, the photon noise contribution, which depends directly on the total optical loading of the telescope and the efficiency of the detectors, is both difficult to accurately predict and, in the case of SPEED, dominates in most channels. In the calculations which follow we make the following assumptions about the LMT and the efficiency of the detectors:

1. Assume effective 30K loading from LMT primary mirror, subreflector, and spillover.
2. Assume 3 mirrors in the re-imaging optics, each at 300K with 2% emissivity.

3. Assume atmosphere with 2mm precipitable H₂O (median value at LMT site).
4. Assume system bandpasses as predicted in Section 2.1.4.
5. Assume optical efficiency = 0.5 times prediction in Section 2.1.4.

One key tradeoff in the use of TES bolometers is in the choice between detector sensitivity (which degrades with the thermal conductivity of the bolometer) and the detector's dynamic range. TES bolometers do not die gracefully. Too great an incident power pushes the thermistor above its superconducting transition and the detector responsivity goes essentially to zero. We therefore choose the bolometer's thermal link such that SPEED will operate under the best calculated optical efficiency and the worst observing conditions we expect to work in at the LMT site - namely, an atmosphere with 8mm precipitable H₂O.

Table 2 gives the resulting optical parameters and sensitivity calculations for all four SPEED bands.

Camera	Frequency [GHz]	N_{pix}	Beamsize [arcsec]	Detector NEP [W/ \sqrt{Hz}]	BLIP [W/ \sqrt{Hz}]	Per-Det. Sensitivity [mJy/ \sqrt{Hz}]
SPEED (LMT)	145	4	12	8e-17	9.22e-17	1.3
	214	4	12	1.2e-16	1.28e-16	2.1
	273	4	12	1.6e-16	1.82e-16	2.7
	375	4	12	1.9e-16	2.33e-16	4.9

Table 2. SPEED Camera Characteristics (on LMT)

These figures include the thermal, Johnson, and photon noise (BLIP) from the radiation load (atmosphere + telescope). A conservative bolometer design is used which degrades the expected sensitivity by a factor of $\sqrt{2}$. Conditions assumed for these calculations are listed in the text.

5. SCIENCE APPLICATIONS

With high sensitivity and simultaneous measurements in four frequency bands, the SPEED camera on the LMT will offer a new and efficient window into several astronomical and cosmological sources. A small sample of these include:

Measurements of the Sunyaev-Zel'dovich Effect in X-ray Clusters

The Sunyaev-Zel'dovich effect (SZE) results when 2.7K CMBR photons are boosted in temperature by Compton up-scattering by hot electrons in the IGM of a cluster of galaxies. The distinct signature of the effect is an increment in the observed CMB temperature at frequencies above 200GHz and a corresponding decrement in temperature at lower frequencies.¹⁴ Measurements of the SZE, in conjunction with measurements of the cluster temperature obtained by x-ray observations, provide a strong constraint on the Hubble Constant and on the star formation history of the universe. SPEED on the LMT is ideally suited for measurements of the SZ effect since it allows simultaneous measurements of the increment, decrement, and nulls in the temperature providing an unambiguous detection of the source of the effect and its magnitude (see Figure 5).

Measurements of Photometric Redshifts of Protogalaxies

A key factor in understanding the evolution of galaxies formed since $z=10$ is the determination of the redshifts of protogalaxies detected by SCUBA and in the future by the BOLOCAM II surveys on the LMT.¹⁵ SPEED is well equipped to play a significant role in this determination. Coupled with IR and FIR measurements of the sources, measurements with the SPEED camera will sample a critical and luminous part of the protogalaxies SED. Figure 6 shows the measured SED of CFRS14A (points) along with a template SED¹⁶ (line) at $z=2.06$. The 5σ sensitivity of SPEED on the LMT after 4 minutes of integration is shown with short thick bars between 100 and 400 GHz. The higher frequency bars are the 5σ sensitivities of the SWIRE SIRTf Legacy Survey and the low frequency bar (at ~ 1 GHz) is the 5σ sensitivity of the deep VLA surveys. Together, these measurements can be used to quickly obtain an estimate of the photometric redshift of the galaxy. The right panel in the figure shows the accuracy of this technique as applied to a small sample of galaxies.¹⁶

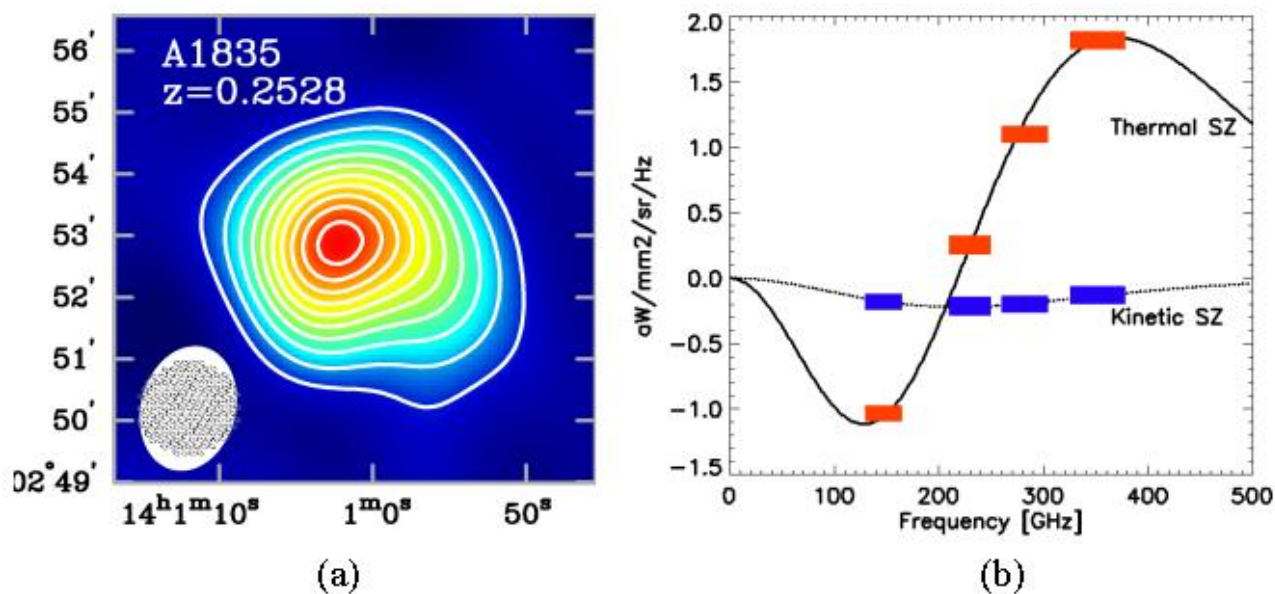


Figure 5. Measuring the SZ Effect

(a) The SZ emission of A1835.² The synthesized beam used to make the map of the SZ is shown in the lower-left corner (open white area). The 144 element BOLOCAM II/LMT footprint is shown inside of this beam. (b) Sample spectra for the thermal and kinetic SZ effects for a cluster with $y = 1 \times 10^{-4}$, $v_c = 500 \text{ km/s}$, and $\tau_e = 0.01$. Overplotted are the predicted 5σ SPEED per-pixel errors after 4 minutes of integration for the thermal and kinetic effects. BOLOCAM II on the LMT will detect clusters by mapping large areas of sky in a single passband. The SPEED camera will make observations in all four passbands shown simultaneously.

Measurement of the Small Angular Scale CMB Anisotropy

At small angular scales (less than a few arcminutes) the CMB anisotropy is suppressed by the duration of the recombination epoch and by any intervening ionization of the universe since recombination. Once again, SPEED is well suited for CMB studies. The multi-frequency nature of the observations provides a direct check for contamination of the CMB signal by foreground sources and the high sensitivity of the detectors allows for high signal-to-noise determinations of the CMB power spectrum at angular scales out of reach of contemporary CMB missions.

5.0.1. Additional Applications of the Ground-Based FSB Instrument

In addition to these applications, SPEED will be used to:

1. construct local universe galaxy templates,
2. identify and image the cold dust in galaxies,
3. perform a survey of dust emission of the inner galaxy,
4. image the dust emission from nearby star forming regions,
5. identify and image comets in the mm continuum,
6. detect asteroids, and
7. study dust emission from disks around young stellar objects.

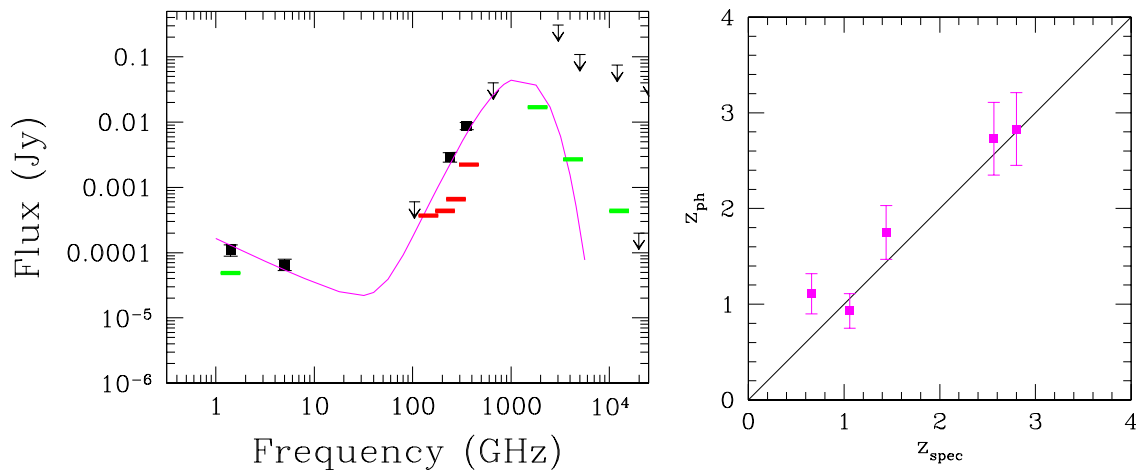


Figure 6. The Measured SED of CFRS14A and the Comparison of Spectroscopic and Photometric redshifts - (Left) FIR, radio and submm spectral energy distribution (points) of source CFRS14A compared with the dusty starburst template¹⁶ (line) at redshift $z = 2.06$. The 5σ sensitivity of SPEED on the LMT after 4 minutes of integration is shown with short, thick bars near 100 GHz. (Right) The photometric redshifts of five submm galaxies compared with their known spectroscopic redshifts.¹⁶

6. CONCLUSION

The SPEED cameras (both the prototype for the HHT and the final version for the LMT) extend the concept of a focal plane array into a third dimension by adding multi-spectral band sensitivity to each pixel in the array. By carefully controlling both stray radiation and the out of band absorption of the detectors, SPEED will attain significantly higher per-detector sensitivity than conventional bolometer arrays by enabling a thorough removal of atmospheric fluctuation noise through both temporal and spatial techniques.

The FSB concept shows great promise for both sub-orbital or orbital payloads where the compact and light-weight aspects of an FSB array can be used to minimize the focal plane volume. The SPEED cameras will be the first achievement of a scientifically active FSB array. The science applications for SPEED on both the HHT and the LMT are diverse and plentiful. The final design for SPEED is nearly complete and we anticipate first light on the HHT in the winter of 2003.

ACKNOWLEDGMENTS

The authors wish to thank Min Yun and the rest of the LMT team for many helpful discussions. This work is supported in part by the LMT Project as well as the NASA Office of Space Science.

REFERENCES

1. D. Hughes, S. Serjeant, J. Dunlop, R. Rowan-Robinson, A. Blain, R. Mann, and R. Ivison, "High-redshift star formation in the hubble deep field revealed by a submillimetre-wavelength survey," *Nature* **394**, p. 241, 1998.
2. J. Carlstrom, M. Joy, L. Grego, G. Holder, W. Holzapfel, S. LaRoque, J. Mohr, and E. Reese, "The sunyaev-zel'dovich effect: Results and future prospects," 2001. in press, preprint astro-ph/0103480.
3. Atmosphere AT Code written by Erich Grossman, 1989.
4. M. S. Kowitt, D. J. Fixsen, A. Goldin, and S. S. Meyer, "Frequency selective bolometers," *Appl. Opt.* **35**, p. 5630, 1996.
5. D. Cottingham, A. Bier, B. Campano, T. Chen, E. Cheng, T. Crawford, F. Finkbeiner, D. Fixsen, D. Logan, S. Meyer, E. Sharp, R. Silverberg, and G. Wilson, "Development of frequency selective bolometers for ground-based mm-wave astronomy," *these proceedings*, 2002.

6. D. J. Benford, C. A. Allen, J. A. Chervenak, M. M. Freund, A. S. Kuttyrev, S. H. Moseley, R. A. Shafer, and J. G. Staguhn, "Multiplexed readout of superconducting bolometers," *Int. J. IR MM Waves* **21**, p. 1909, 2000.
7. J. A. Chervenak, K. D. Irwin, E. N. Grossman, J. M. Martinis, C. D. Reintsema, and M. E. Huber, "Superconducting multiplexer for arrays of transition edge sensors," *Appl. Phys. Lett.* **74**, p. 4043, 1999.
8. E. Archibald, T. Jenness, W. Holland, I. Coulson, N. Jessop, J. Stevens, E. Robson, R. Tilanus, W. Duncan, and J. Lightfoot *Monthly Notices of the Royal Ast. Soc.* , 2002. in press, preprint astro-ph/0204444.
9. P. Mauskopf Private communication, 2002.
10. S. S. Meyer, A. D. Jeffries, and R. Weiss, "A search for the sunyaev-zel'dovich effect at millimeter wavelengths," *Astrophys. J. Letters* **271**, p. L1, 1983.
11. J. C. Mather, "Bolometer noise: nonequilibrium theory," *Appl. Opt.* **21**, p. 1125, 1982.
12. J. C. Mather, "Bolometers: ultimate sensitivity, optimization, and amplifier coupling," *Appl. Opt.* **23**, p. 584, 1984.
13. S. Lee, J. M. Gildemeister, W. Holmes, A. T. Lee, and P. L. Richards, "Voltage-biased superconducting transition-edge bolometer with strong electrothermal feedback operated at 370 mK," *Appl. Opt.* **37**, pp. 3391–3397, June 1998.
14. R. A. Sunyaev and Y. B. Zel'dovich *Ap. & Sp. Sci.* **7**, p. 3, 1970.
15. C. L. Carilli and M. S. Yun, "The radio-to-submillimeter spectral index as a redshift indicator," *Astrophys. J. Letters* **513**, pp. L13–L16, Mar. 1999.
16. M. Yun and C. Carilli *Astrophys. J.* , 2002. in press, preprint astro-ph/0103480.